EFFECT OF Cu-EXCESS ON THREE-STAGE CuGaSe$_2$ THIN FILMS USING IN-SITU PROCESS CONTROLS

R. Caballero[*], S. Siebentritt, K. Sakurai[+], C.A. Kaufmann, H.W. Schock, M. Ch. Lux-Steiner

Hahn-Meitner-Institut Berlin GmbH, Glienickerstrasse 100, 14109 Berlin, Germany

ABSTRACT

The objective of this work is to study the effect of Cu-excess and compare the growth mechanism of CuGaSe$_2$ (CGS) films coevaporated using a bilayer and a three-stage process and evaluate the consequences of the latter for CGS on transparent back contacts. CGS thin films are prepared by coevaporation in a three-stage process onto Mo/soda-lime substrates and onto FTO. In contrast to the bilayer process, Cu-Se phases are only observed on the surface at the end of the second stage, e$_2$. This allows to work with a broader Cu-excess window. Atomic ratios (Cu/Ga)e$_2$ of around 1.3 at the end of deposition phase 2 in the three-stage process show the better device efficiencies due to a larger grain formation. Increasing the Cu-content leads to a slight decrease of the grain size and voids are observed in the film, reducing the FF of the device. The CGS morphology and the solar cells efficiency are dominated by the Cu excess more than by the T$_{substrate}$ between 535° C and 500° C. Similar results are obtained for CGS on FTO: (Cu/Ga)e$_2$ ~1.3 as best composition at T$_{substrate}$=500° C.

Keywords: CuGaSe$_2$; three-stage process; bilayer process

1. INTRODUCTION

An efficiency higher than 25 % of thin-film tandem solar cells is predicted as a very attractive way forward in the photovoltaic technology [1]. $CuGaSe_2$ (CGS) with a band gap of 1.7 eV is one of the ideal compounds to be used as the top cell for a tandem photovoltaic device. Different processes for preparing CGS films have been proposed, such as the bilayer and the three-stage process [2,3]. The three-stage process has produced the best device efficiencies to date [4]. In the bilayer process, the first stage consists of deposition of Cu, Ga and Se forming Cu-rich CGS films. In the second stage, the precursor layer is exposed to Ga and Se fluxes only in order to form Ga-rich CGS films. Nishiwaki et al. [2] have observed a decrease of V_{OC} and the grain size with the Cu excess because of Cu-Se grains between CGS grains. These copper selenide grains are present at the film surface, and some extend through the entire film down to the Mo [5]. Once the bilayer process was studied and these results were obtained, the three-stage process was implemented in our laboratory. For a better understanding of the differences between both deposition processes, we investigate the growth mechanism of CGS thin films using the three-stage process and compare with the one using the bilayer process.

In order to use the CGS solar cell as the top cell for a mechanically stacked tandem device, a transparent back contact is required. Hence, the effect of the control parameters of the CGS morphology on the optical and electrical properties of the transparent back contact are also studied.

2. EXPERIMENTAL

CGS thin films are grown onto Mo or FTO coated soda lime glass using co-evaporation in a three-stage process, as described elsewhere [6]. Commercially

available FTO with a sheet resistance of 8 Ω/sq and an optical transmission higher than 75 % at 550 nm is used. As sodium does not diffuse through FTO, a NaF layer is deposited onto the transparent back contact prior to the CGS deposition process using physical vapor deposition. It is necessary to supply sodium as it plays a crucial role for high quality absorbers [7].

LLS together with a pyrometer is used as in-situ process control. Laser light scattering and pyrometer have proven to be valuable tools for process control [8,9]. The light source is a 635 nm red laser and the detector is a photomultiplier with lock-in technology. Heat radiation from the sample was monitored by a pyrometer placed with its line of view perpendicular to the substrate surface. The temperature is measured by a thermocouple behind the substrate. The temperatures are given as measured in the experimental set-up and hence depend on several parameters such as for example the position of the thermocouple. Fig. 1 illustrates the three-stage process together with typical results for LLS and the pyrometer profiles and the thermocouple temperature of a CGS process on Mo.

Solar cells with a Ni-Al/ZnO/CdS/CGS/Mo/soda-lime glass or Ni-Al/ZnO/CdS/CGS/FTO/glass structure have been fabricated. The absorber composition is analyzed by X-ray fluorescence (XRF) and energy dispersive X-ray spectroscopy (EDX). The microstructure is studied by scanning electron microscopy (SEM) and transmission electron microscopy (TEM). Solar cell characterization is carried out under AM1.5 illumination, 100 mW/cm^2 intensity at 25⁰ C. The total area of the solar cell devices is 0.5 cm^2.

3. RESULTS AND DISCUSSION

Fig. 1 shows the LLS and pyrometer signals for a co-evaporation process on Mo. Once the first stoichiometric point s_1 is passed, i.e. Cu/Ga>1, the scattered laser light

intensity increases significantly because of the higher roughness of the Cu-rich film. The film temperature from the thermocouple decreases with time during addition of Cu. This is due to a higher emissivity of Cu-Se phases compared to that of stoichiometric CGS or Ga-rich CGS films [10]. The film temperature increases during the third stage and atomic ratio Cu/Ga decreases with third stage time. However, the pyrometer signal indicates the opposite behaviour for the second stage. Once s_1 is passed, the signal starts to increase as does the scaterred laser light intensity. We attribute this to reflections coming from the Cu-source due to not so large distance between the source and the pyrometer position. In Figure 1, the duration (e_2-s_1) is 30 % of duration (s_1-e_1) for both substrates. Once $t_{(e2-s1)} \geq 25\% t_{(s1-e1)}$ during the process on Mo, the increase of the scattered laser light intensity is less steep and the pyrometer signal is more constant. This would indicate a smoother surface when the material is Cu-rich enough. So, LLS and pyrometer profiles allow us to judge the composition and the roughness of the film during the process.

Figure 2 shows the cross-sectional TEM and SEM images of two samples on Mo with different atomic ratios Cu to Ga, (a) and (c) 1.12 and (b) and (d) 1.34. In contrast to the bilayer process [5], EDX within the TEM indicates that almost all the grains are stoichiometric CGS and Cu-Se phases are only located on the surface and no Cu-Se grains are observed in-between CGS grains. It is considered an advantage of the three-stage process, that a broader Cu-excess window is made possible. Moreover, the film in Figure 2c is rougher than that in Figure 2d, what is in agreement with the observations from the LLS and pyrometer signals.

Films with a Ga-rich final composition are prepared from films with different Cu-rich compositions in the second stage of the three-stage process. The composition ratios of Cu to Ga after the second stage, $(Cu/Ga)_{e2}$, are estimated from the final film composition and the duration of the stages assuming constant fluxes. Figure 3 shows

SEM micrographs of the surface of three Ga-rich CGS films, with a constant final composition of Cu/Ga=0.89, prepared from (a) $(Cu/Ga)e_2$=1.16, (b) 1.26 and (c) 1.37 at T_2=535° C. A tendency in the grain size can be observed. The grain growth is improved using Cu-Se as a flux agent. The grain size increases with the Cu-content until $(Cu/Ga)e_2$ around 1.3. It is due to the absence of Cu-Se phases between CGS grains, not obstructing the lateral growth of the CGS grains. At around $(Cu/Ga)e_2$>1.35 the grain size decreases slightly. For extremely high $(Cu/Ga)e_2$~1.4, large voids appear in the CGS film. Similar to the bilayer process, the difference between the growth rate of inherent CGS grains and converting grains during the third stage is deemed to be a reason for the voids in the film. Thus it is found that the amount of Cu excess during the deposition process affects the microstructure of the final CGS films. A similar effect but to another extend has been observed for the bilayer process [5] and for CIS [11]. It is known that the device efficiency depends on the CGS film morphology, which is governed by the Cu-content at the end of the second stage of our process. Table 1 presents the composition, $T_{substrate}$ and PV-parameters of some devices. Different process conditions of CdS and ZnO films have been used, which will be studied in another work. A tendency for a higher efficiency when $(Cu/Ga)e_2$ is around 1.3 is observed and attributed to the largest grains, which are seen to be independent of the conditons of subsequent layers. However, the device efficiency starts to decrease for extremely Cu-rich films after the second stage. The voids observed could be responsible for the decrease in FF (sample 4b in Table 1).

Another factor to take into account during the deposition process is the substrate temperature, $T_{substrate}$. In Figure 4 cross-section SEM pictures of CGS thin films on Mo at different $T_{substrate}$ are displayed. Figure 4a and 4b show samples with a final

atomic ratio Cu to Ga of 0.91 and $(Cu/Ga)e_2=1.16$. As can be observed, $T_{substrate}\cong560°$ C is characterized by a good columnar structure with large grains. Unfortunately, the soda lime glass is bent at that nominal $T_{substrate}$, preventing device fabrication. The grains for the sample of the Figure 4b, $T_{substrate}=535°$ C, are smaller in size, and the image shows a layer of smaller grains toward the back of the film. Therefore, a higher $T_{substrate}$ implies a higher quality of the absorber. However, the morphological differences in the range between 535° C and 500° C are not significant when an appropiate Cu excess is reached during the process. In Figure 4c and 4d, cross-section SEM pictures of CGS films with a final composition of $Cu/Ga=0.89$ with $(Cu/Ga)e_2=1.26$ at 535° C and 500° C respectively are shown. This similar structure is translated into similar solar cell efficiencies in this range of $T_{substrate}$ and no loss in efficiency is observed for the lowest $T_{substrate}$. This indicates that the Cu content is the dominant factor at the end of the second stage (see Table 1). It is again observed that a smaller grain size for the lower Cu excess is present in Figure 4b and Figure 4c. But a decrease of $T_{substrate}<500°$ C leads to a reduction of the device efficiency because of a less compact structure and the decrease of grain size. This is likely due to a lower surface mobility during the growth at lower temperatures [12] and indicates the importance of a reasonably high $T_{substrate}$ to maintain a sufficient quality of the absorber. So, it is expected to achieve enhanced efficiencies for solar cells on Mo combining a high $T_{substrate}$ (>535° C) and an optimum Cu excess during the process $((Cu/Ga)e_2 \sim 1.3)$.

3.1. Consequences for CGS on FTO

In order to use the CGS solar cell as the top cell of a tandem device, it is necessary, apart from an enhaced efficiency, to achieve a high optical transmission (T_{opt}) for long wavelengths. The Cu-content at the end of the second stage also affects the optical

transmission of the solar cell on FTO. A high $(Cu/Ga)e_2$ leads to a considerable reduction of the T_{opt} [6]. It could be in part attributed to the slight decrease of grain size, which has been also observed on Mo. Moreover, an increase of $(Cu/Ga)e_2$ up to 1.35 leads to an increased solar cell efficiency because of the decreased resistivity of the FTO [6] .

As it has been observed, using $(Cu/Ga)e_2 \sim 1.3$ allows to reduce $T_{substrate} < 535°$ C without decreasing the efficiency of the device. But the electrical properties of the transparent back contact are strongly influenced by the process temperature. $T_{substrate} < 520°$ C is necessary to avoid a high increase of the FTO resistivity after the absorber process, which leads to a low FF of the device due to a high series resistance. So far $T_{substrate} = 500°$ C has led to the best results in our process to date, 4.2 % of efficiency [6].

4. CONCLUSIONS

In contrast to observation made for the bilayer process, in the three-stage process the grain size increases with the Cu excess that is reached at the end of the second stage. This is due to the fact that no Cu-Se grains are observed in-between CGS grains, but only at films surface. It proves benificial to increase the Cu excess up to around 1.3. However, large voids appear in CGS films for extremely Cu-rich composition at the end of the second stage. Choosing the correct composition, $(Cu/Ga)e_2 \sim 1.3$, the process window for $T_{substrate}$ remains between 535° C and 500° C and is an uncritical factor. The amount of Cu excess affects the microstructure of the films, which dominates the solar cells efficiency. CGS solar cells on FTO present a similar behaviour as those on Mo: $(Cu/Ga)e_2 \sim 1.3$ as best composition at the end of deposition phase 2 and $T_{substrate} \sim 500 °$ C.

Acknowledgments

REFERENCES

[1] T.J. Coutts, J.S. Ward, D.L. Young, K.A. Emery, T.A. Gessert, R. Noufi, Prog. Photovolt: Res. Appl. 11 (2003) 359.

[2] S. Nishiwaki, M. Giersig, S. Schuler, M. Dziedzina, S. Siebentritt, M. Ch. Lux-Steiner, Proceedings of the 17th Photovoltaics Specialists Conference, Munich, Germany, 2001, p. 1147.

[3] A.M. Gabor, J.R. Tuttle, M.H. Bode, A. Franz, A.L. Tennant, M.A. Contreras, R. Noufi, D.G. Jensen, A. Hermann, Sol. Energy Mater. Sol. Cells 41/42 (1996) 247.

[4] J. AbuShama, R. Noufi, S. Johnston, S. Ward, X. Wu, Proceedings of the 31st IEEE Photovoltaic Specialists Conference and Exhibition, Florida, USA, 2005, p.

[5] S. Nishiwaki, S. Siebentritt, M. Giersig, M. Ch. Lux-Steiner, J. Appl. Phys., Vol. 94, No. 10 (2003) 6864.

[6] R. Caballero, S. Siebentritt, K. Sakurai, C.A. Kaufmann, M. Ch. Lux-Steiner, Proceedings of the IEEE 4th World Conference on Photovoltaic Energy Conversion, Waikoloa, Hawaii, USA, May 2006.

[7] K. Granath, M. Bodegard, L. Stolt, Sol. Energy Mater. Sol. Cells 60/3 (2000) 279.

[8] K. Sakurai, R. Hunger, R. Scheer, C.A. Kaufmann, A. Yamada, T. Baba, Y. Kimura, K. Matsubara, P. Fons, H. Nakanishi, S. Niki, Prog. Photovolt: Res. Appl. 12 (2004) 219.

[9] C.A. Kaufmann, A. Neisser, R. Klenk, R. Scheer, Thin Solid Films 480-481 (2005) 515.

[10] N. Kohara, T. Negami, M. Nishitani, T. Wada, J.J. Appl. Phys 34 (1995)1141.

[11] R. Klenk, T. Walter, H.W. Schock, D. Cahen, Adv. Mater. (Weinheim, Ger.) 5 (1993) 144.

[12] L. Maissel, R. Glang, Handbook of Thin Film Technology, McGraw-Hill, USA, 1970, p. 8-40.

Table 1. Composition, $T_{substrate}$ and PV-parameters of different solar cells

Sample	Cu/Ga	$(Cu/Ga)e_2$	Back contact	$T_{substrate}$ (°C)	V_{oc} (mV)	J_{sc} (mA/cm^2)	FF (%)	η (%)
1a	0.91	1.19	Mo	535	838	13.4	44.3	5.0
1b	0.89	1.26	Mo	535	837	14.5	51.5	6.3
2a	0.89	1.25	Mo	535	872	13.3	54.4	6.3
2b	0.89	1.37	Mo	535	818	11.1	50.6	4.6
3a	0.89	1.25	Mo	535	829	14.3	54.9	6.5
3b	0.89	1.37	Mo	535	896	13.1	49.9	5.9
4a	0.89	1.26	Mo	535	753	16.1	60.5	7.3
4b	0.91	1.40	Mo	535	671	15.0	47.6	4.8
5a	0.97	1.32	Mo	520	711	14.4	64.1	6.6
5b	0.89	1.25	Mo	500	790	14.2	57.8	6.5
5c	0.89	1.35	Mo	500	786	14.6	57.4	6.6
5d	0.92	1.24	Mo	490	656	11.7	60.7	4.7

Note: The same number of the sample indicates that the CdS and ZnO layers are made under the same conditions

Figure Captions

Figure 1. Pyrometer and laser light scattering signal transients, the thermocouple temperature and the flux schematics for a three-stage $CuGaSe_2$ process on Mo .

Figure 2. Cross-sectional transmission electron microscopy (a,b) and scanning electron microscopy (c,d) images of $CuGaSe_2$ on Mo after the second stage with (a,c) $(Cu/Ga)e_2$=1.12 and (b,d) $(Cu/Ga)e_2$=1.34

Figure 3. Scanning electron micrographs of $CuGaSe_2$ films with Cu/Ga=0.89 prepared from $(Cu/Ga)e_2$ (a) 1.16, (b) 1.26, (c) 1.37

Figure 4. Cross-sectional scanning electron microscopy images of $CuGaSe_2$ on Mo at $T_{substrate}$ of (a) 560º C and (b) 535º C with Cu/Ga=0.91 and $(Cu/Ga)e_2$=1.16 and of (c) 535° C and (d) 500° C with Cu/Ga=0.89 and $(Cu/Ga)e_2$=1.26
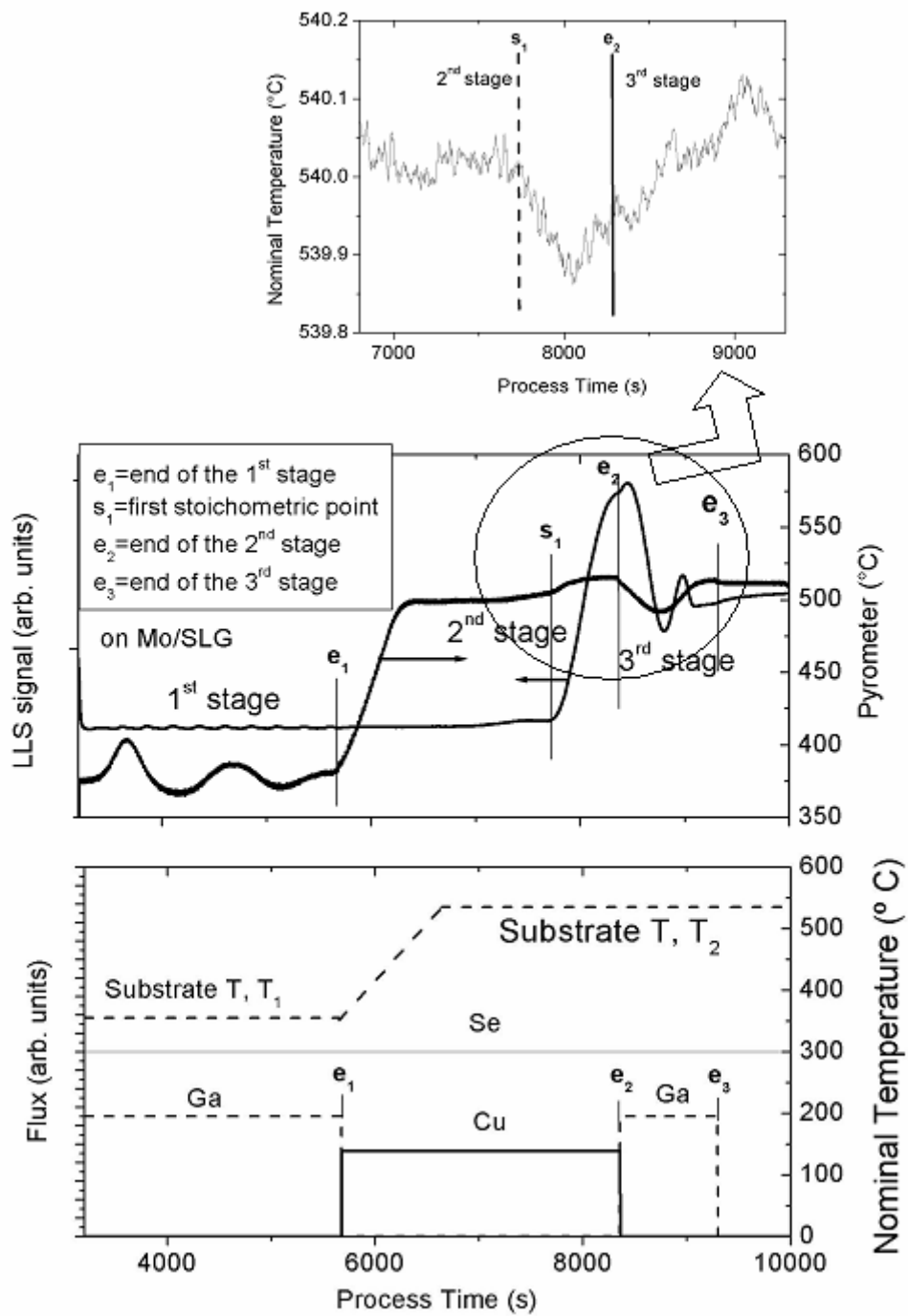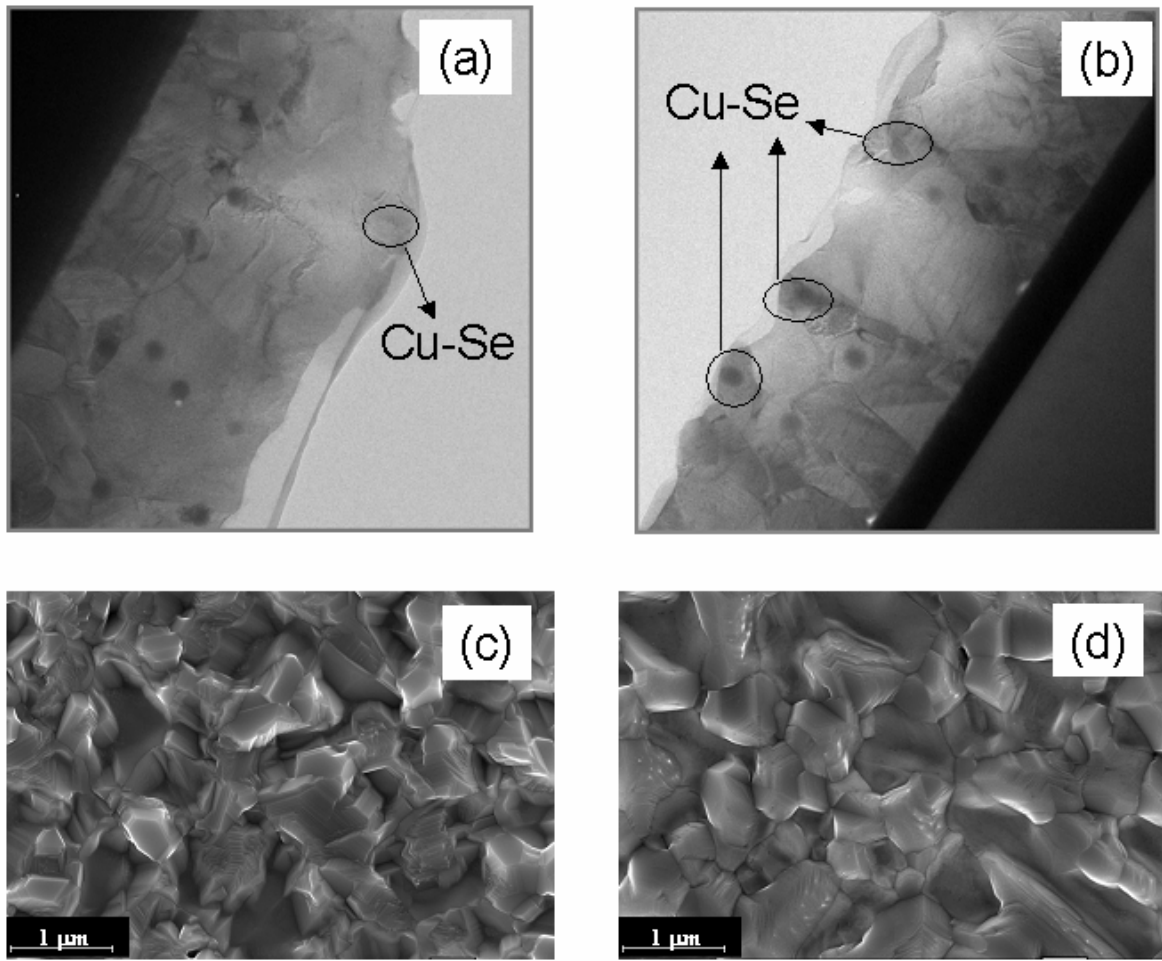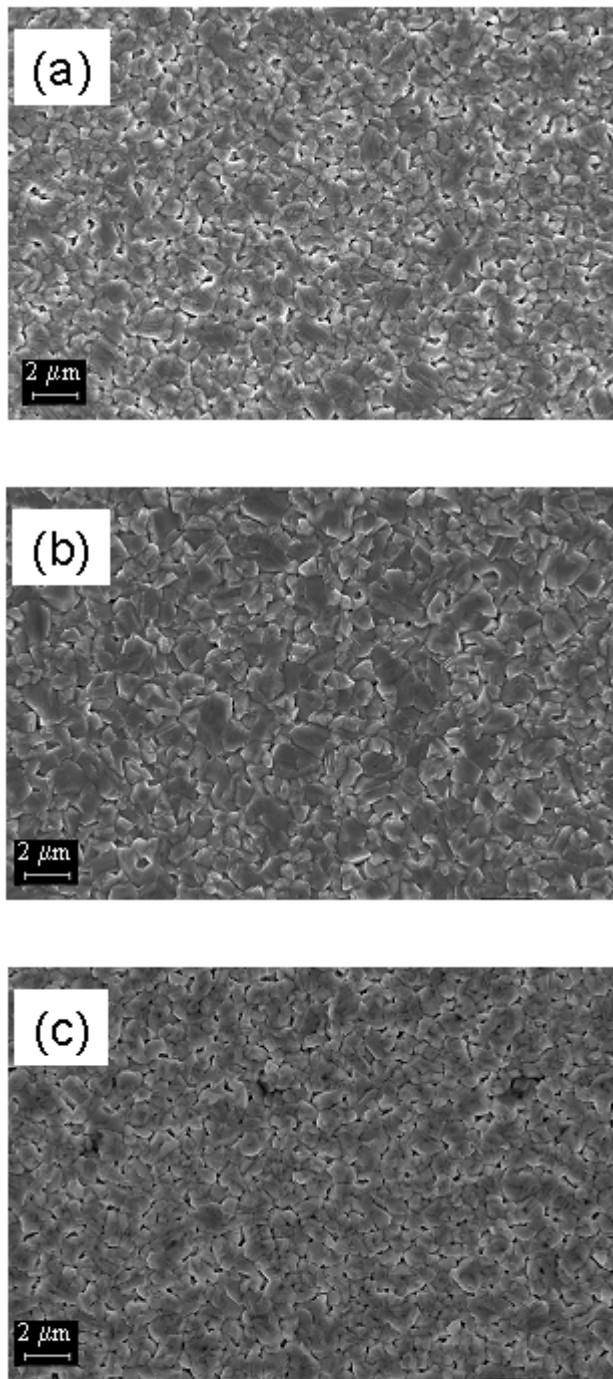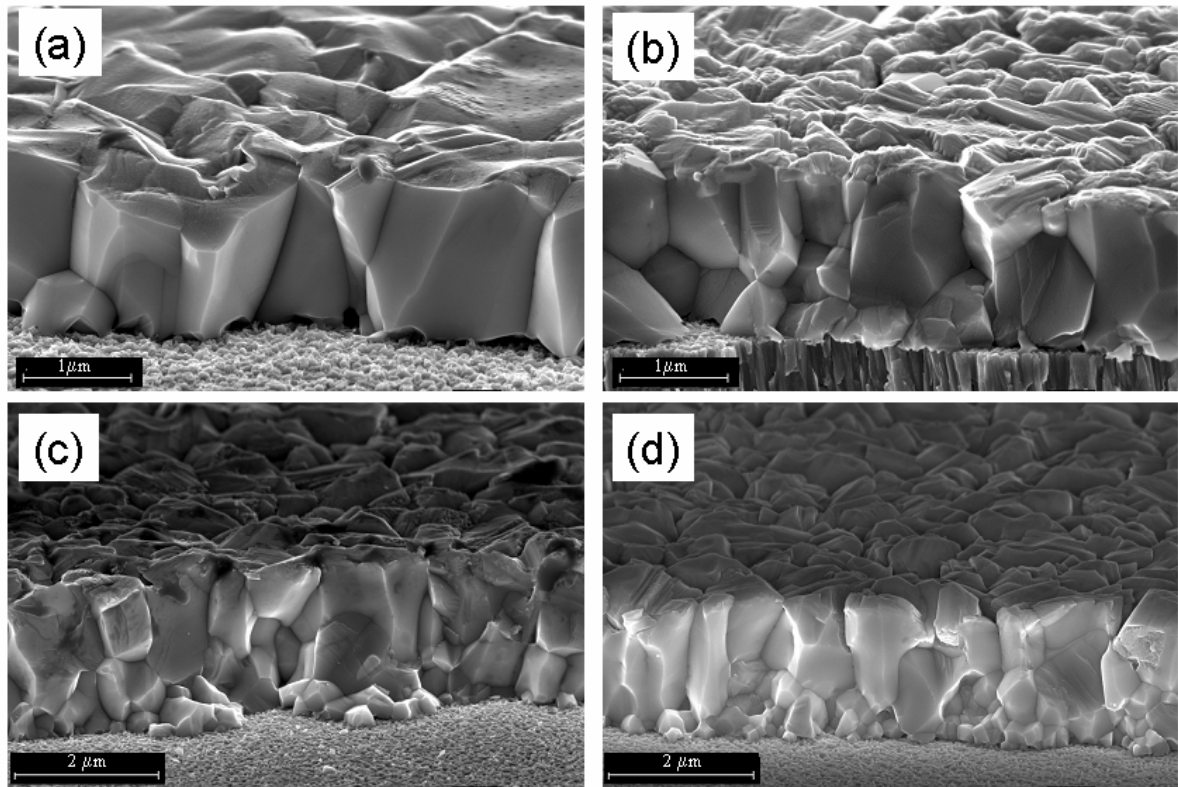
Figure 1

Figure 2

Figure 3

Figure 4